Fluid Mechanical Matching of H^+-ATP Synthase Subunit *c*-Ring with Lipid Membranes Revealed by ^2H Solid-State NMR

Masatoshi Kobayashi,*§ Andrey V. Struts,† Toshimichi Fujiwara,* Michael F. Brown,†‡ and Hideo Akutsu*§
*Institute for Protein Research, Osaka University, Yamadoaka, Suita 565-0871, Japan; †Department of Chemistry and ‡Department of Physics, University of Arizona, Tucson, Arizona 85721; and §Core Research of Evolutional Science and Technology, Japan Science and Technology Agency, Japan

ABSTRACT The F_1F_o-ATP synthase utilizes the transmembrane H^+ gradient for the synthesis of ATP. F_o subunit *c*-ring plays a key role in transporting H^+ through F_o in the membrane. We investigated the interactions of *Escherichia coli* subunit *c* with dimyristoylphosphatidylcholine (DMPC-d_{54}) at lipid/protein ratios of 50:1 and 20:1 by means of ^2H-solid-state NMR. In the liquid-crystalline state of DMPC, the ^2H-NMR moment values and the order parameter (S_{CD}) profile were little affected by the presence of subunit *c*, suggesting that the bilayer thickness in the liquid-crystalline state is matched to the transmembrane hydrophobic surface of subunit *c*. On the other hand, hydrophobic mismatch of subunit *c* with the lipid bilayer was observed in the gel state of DMPC. Moreover, the viscoelasticity represented by a square-law function of the ^2H-NMR relaxation was also little influenced by subunit *c* in the fluid phase, in contrast with flexible nonionic detergents or rigid additives. Thus, the hydrophobic matching of the lipid bilayer to subunit *c* involves at least two factors, the hydrophobic length and the fluid mechanical property. These findings may be important for the torque generation in the rotary catalytic mechanism of the F_1F_o-ATPse molecular motor.

INTRODUCTION

The F_1F_o-ATP synthase is a ubiquitous molecular motor involved in H^+-mediated energy conversion. It is found in a variety of organisms from bacteria to humans. The H^+-driven ATP synthase converts the energy of the transmembrane electrochemical potential to ATP. It consists of a water-soluble F_1 portion and a membrane-integrated F_o portion. The former has catalytic sites for ATP synthesis and hydrolysis, and the latter mediates H^+ transport across the membrane (1,2). The F_1 and F_o domains consist of multiple subunits $\alpha_3\beta_3\gamma\delta\varepsilon$ and ab_2c_n, respectively. The rotary motor contains an ion-binding rotor ring embedded in the membrane bilayer. The rotor ring in F_o consists of an oligomeric assembly of subunit *c*. The rotor ring of the F-type H^+-ATP synthase has been well studied by biochemical approaches (3–5), including investigations of biological activity that is affected by various genetic modifications. Recently, the ring structures of the F-type and V-type Na^+-ATPase have been reported (6,7). Structural studies of *c*-ring of H^+-ATP synthase have been performed with atomic force microscopy and cryo-transmission electron microscopy (8,9), and the ion translocation mechanism has been discussed on the basis of these studies. The oligomeric subunit *c*-ring structure interacts with subunit *a*, which is located outside the *c*-ring. Proton movements through F_o are reversibly coupled to ATP synthesis or its hydrolysis. Protons are thought to be translocated through subunits *a* and *c*.

A conformational change of the C-terminal helix on deprotonation of the essential residue Asp-61 was found in a solution NMR study of monomeric subunit *c* in organic solvent (10). A rotational mechanism by the helix twisting coupled with H^+-translocation was proposed on the basis of this observation. On the other hand, Nakano et al. reported a new structure of subunit *c* indicating that deprotonation of the essential Asp-61 residue of subunit *c* does not induce large conformational change. They proposed that side-chain flipping coupled with the membrane potential drives the rotation of the *c*-ring (11). A Brownian ratchet model has also been proposed on the basis of thermal fluctuations of the ring (12).

To understand the rotary catalytic mechanism of the molecular motor, investigations on interactions of the rotor with the membrane lipid bilayer are also important. Since subunit *c* is deeply embedded in the bilayer, lipid-protein interactions could play an important role not only in mechanical support of F_o but also in generating the torque in the rotary mechanism. We applied solid-state ^2H-NMR spectroscopy to obtain information on interaction of the *Escherichia coli* F_o *c*-ring with the membrane lipid bilayer in relation to the molecular mechanism of the force generation, using dimyristoylphosphatidylcholine with perdeuterated acyl chains (DMPC-d_{54}). Although the real membranes contain not only the saturated fatty acids but also unsaturated ones, DMPC can be used as a model in terms of physicochemical properties at ambient temperatures (13). Our results reveal that hydrophobic matching of subunit *c* to the thickness of the bilayer hydrocarbon region occurs in the L_α state despite the significant mismatch in the gel state. The influence of subunit *c* on the lipid properties in the L_α phase was examined through measurement of the order parameters and spin-lattice (R_{1Z}) relaxation rates using ^2H-NMR. Its influences on the bilayer elasticity were evident but rather small in

Submitted October 10, 2007, and accepted for publication January 22, 2008.

Address reprint requests to Hideo Akutsu, Institute for Protein Research, Osaka University, 3-2 Yamadaoka, Suita, Osaka 565-0871, Japan. Tel.: 81-6-6872-8218; Fax: 81-6-6872-8219; and E-mail address: akutsu@protein.osaka-u.ac.jp.

Editor: Arthur G. Palmer III.

0006-3495/08/06/4339/09 $2.00

doi: 10.1529/biophysj.107.123745

contrast to other additives such as cholesterol and detergents. Implications of these findings for the rotary mechanism coupled with H^+ translocation in H^+-ATP synthase are discussed.

MATERIALS AND METHODS

Expression and purification of F_1F_o-ATP synthase subunit c

E. coli (MEG119 strain) cells transformed by a plasmid carrying the gene for *E. coli* subunit *c* (pCP35) were cultured in LB (Luria-Bertani broth) for 24–26 h. Purification of subunit *c* was carried out according to the reported method (14,15). The collected cells (wet 27.2 g) were suspended in the same volume of a 100 mM sodium acetate buffer and were homogenized by sonication on ice. Subunit *c* was extracted from them with 12 wet cell volumes of a chloroform/methanol (1:1) mixture for 2 h at 4°C. The supernatant was collected after centrifugation. Chloroform and water were added to the supernatant. The resultant chloroform/methanol/water (8:4:3) mixture was left standing still overnight at 4°C. The chloroform fraction was collected and concentrated to 2–4 mL with a rotary evaporator. Then, subunit *c* was precipitated with the addition of 5 volumes of diethyl ether at −30°C for 2 days. The crude subunit *c* was applied to a carboxymethyl cellulose column and was eluted with a chloroform/methanol/water (5:5:1) solution. The yield was ~10 mg/4 L of culture. The purity of the subunit *c* was confirmed by Tricine sodium dodecylsulfate-polyacrylamide gel electrophoresis (SDS-PAGE) and matrix-assisted laser desorption ionization time-of-flight mass spectrometry with a matrix-assisted laser desorption ionization time-of-flight mass spectrometer (Autoflex, Bruker Daltonics, Bremen, Germany). The latter gave the mass number of 8299, which is within experimental error of the theoretical mass number of 8284 for formylated subunit *c*.

Preparation and characterization of reconstituted membranes

1,2-diperdeuteriomyristoyl-*sn*-glycero-3-phosphocholine (DMPC-d_{54}) was obtained from Avanti Polar Lipids (Alabaster, AL). Silica gel thin-layer chromatography developed with $CHCl_3$/MeOH/H_2O (65:35:5) gave a single spot. First, 5 mg of subunit *c* was dissolved in 10 mL of deionized water containing ~40 mM octyl-β-D-glucoside (OG) (critical micelle concentration, 25 mM). The solution was visually translucent. Then, DMPC-d_{54} was added to the solution at a 1:50 or 1:20 protein/lipid molar ratio. It was dialyzed for 4 days against 5 L of buffer solution (200 mM NaCl, 1 mM NaN_3, 10 mM Tris-HCl, pH 8.0) at 26°C (above the main lipid phase transition temperature), using dialysis tubing with an 8000 molecular weight cutoff (Nacalai Tesque, Kyoto, Japan). NaCl was omitted from the final dialysis buffer solution to suppress the conductivity of the samples. The reconstituted membranes were collected by centrifugation at 5000 rpm (6100 × *g*) in a 50 mL Falcon tube.

The precipitated membranes were suspended in 1–2 mL of buffer. To form homogeneous liposomes, freeze-thaw cycles (30°C, 4°C, and −30°C for 20 min at each temperature) were repeated more than 10 times. The liposome suspension was then transferred to a 1.5 mL Eppendorf tube. To suppress the natural abundance signal, water was replaced by a ^{2}H-depleted one (CEA-ORIS; Bureau des Isotopes Stables, Paris, France) through washing three times. The presence and stability of the subunit *c* was confirmed by Tricine SDS-PAGE after the experiments. A control sample of reconstituted membranes containing subunit *c* was prepared in exactly the same way using nonlabeled DMPC. It was applied to a sucrose density-gradient centrifugation at 28,000 rpm (103,500 × *g*) for 16 h at 4°C. A single predominant band corresponding to the proteolipid membrane was observed, suggesting that prepared sample was homogeneous. Pure DMPC liposomes gave a distinctly different band in the lighter density region. Therefore, the membranes should be properly reconstituted.

Analytical ultracentrifugation of subunit *c* in OG solution (1 mg/mL) above the critical micelle concentration was performed with a Beckman Optima XL-A centrifuge at 20°C (Beckman, Fullerton, CA). Sedimentation velocity and sedimentation equilibrium experiments were carried out at 35,000 rpm for 1 h and at 12,000 rpm for 24 h, respectively. Protein concentration in the cell was scanned using an ultraviolet light at 280 nm.

Solid-state ^{2}H- and ^{31}P-NMR spectroscopy

NMR measurements were performed with a Varian (Palo Alto, CA) Infinity-plus 500 spectrometer operating at 11.74 T static magnetic field (^{2}H- and ^{31}P-frequencies, 76.705 and 202.277 MHz, respectively). For static ^{2}H- and ^{31}P-NMR experiments, a 3.2 mmϕ magic-angle spinning (MAS) probe was used. A glass NMR tube (3 mmϕ, Shigemi; Tokyo, Japan) was cut and used as a sample tube with a Teflon cap. The sample volume was 35–40 μL. The position of the sample was carefully adjusted to minimize the $\pi/2$ pulse length, which was 3.57 μs, corresponding to $\gamma B_1/2\pi = 70$ kHz. The quadrupolar echo sequence was used for ^{2}H-NMR measurements with a 30 μs pulse spacing period τ. The spectral width was 1.0 MHz, and the recycle delay was 1.0 s for the samples in the liquid-crystalline state and 0.5 s for the gel state. The number of acquisitions was 4000–12,000. The ^{2}H-spin-lattice relaxation (Zeeman) rates (R_{1Z}) of the DMPC-d_{54} reconstituted membranes were measured in the liquid-crystalline state using a combination of quadrupolar echo and inversion recovery pulse sequences, $(\pi)_x - t - (\pi/2)_x - \tau - (\pi/2)_y - \tau -$ acquisition. Pulses were appropriately phase-cycled and delay times t ranged 0.2–1 s, depending on the T_{1Z} relaxation time of the sample. ^{31}P-spectra were obtained with a single pulse under two-pulse-phase-modulation ^{1}H-decoupling at 30°C. The $\pi/2$ pulse length was 5 μs. The number of acquisitions was 10,000.

Reduction and analysis of ^{2}H-NMR data

^{2}H-NMR spectral powder patterns were numerically deconvoluted (de-Paked) to yield the spectra for the orientation at $\theta = 0°$ as described (16,17). Order parameters were determined from the observed residual quadrupolar couplings (RQCs; $\Delta\nu_Q$) according to

$$\left|\Delta\nu_Q^{(i)}\right| = \frac{3}{2}\chi_Q\left|S_{CD}^{(i)}\right|\left|P_2(\cos\theta)\right|. \quad (1)$$

Here $\chi_Q = e^2qQ/\hbar$ represents the static quadrupolar coupling constant (167 kHz for ^{2}H in the C–^{2}H-bond; 18), $S_{CD}^{(i)} = 1/2\langle 3\cos^2\beta_i - 1\rangle$ is the segmental order parameter, and P_2 is the second Legendre polynomial, where θ is the angle between the bilayer director axis and the main external magnetic field $\mathbf{B_0}$. For the de-Paked ^{2}H-NMR spectra ($\theta = 0°$), $P_2(\cos\theta) = 1$. The Pake doublets are assigned beginning with the terminal methyl group, which exhibits the smallest quadrupolar splitting. The methylene groups were assigned consecutively according to their increasing quadrupolar splittings.

Half-moments (M_k) of the powder-type spectra were calculated using the equation

$$M_k = \frac{\int_0^\infty \omega^k f(\omega)d\omega}{\int_0^\infty f(\omega)d\omega}, \quad (2)$$

where $f(\omega)$ is the spectral intensity at frequency ω. The kth moment is related to the distribution of the segmental order parameters by

$$M_k = A_k\left(\frac{3\pi}{2}\right)\chi_Q\frac{1}{n_C}\sum_{i=2}^{n_C}\left|S_{CD}^{(i)}\right|^k, \quad (3)$$

where A_k is a constant proportional to k (18,19). The moments are useful for a qualitative characterization of the bilayer order, particularly in the gel state where quadrupolar splittings due to individual carbon segments are not resolved. The first moment (M_1) is proportional to the mean value of S_{CD} over all the acyl chain segments:

$$M_1 = \left(\frac{\pi}{\sqrt{3}}\right)\chi_Q\frac{1}{n_C}\sum_{i=2}^{n_C}\left|S_{CD}^{(i)}\right| = \frac{\pi}{\sqrt{3}}\chi_Q\langle|S_{CD}|\rangle, \quad (4)$$

and the second moment (M_2) is proportional to the average value of the squared order parameter:

$$M_2 = \left(\frac{9\pi^2}{20}\right)\chi_Q^2 \frac{1}{n_C}\sum_{i=2}^{n_C}\left|S_{CD}^{(i)}\right|^2 = \frac{9\pi^2}{20}\chi_Q^2\langle|S_{CD}|^2\rangle. \quad (5)$$

Calculation of structural parameters

From the $S_{CD}^{(i)}$ order profiles, the thickness of the hydrocarbon region D_C can be calculated (20). The equilibrium or average chain length is described by a set of virtual bond vectors attached to each of the segments, which are perpendicular to the methylene ^{2}H–C–^{2}H plane and have a length of $l_0 = 1.27$ Å (21–24). The most important quantity for calculating the structural parameters is the instantaneous travel of each carbon segment i along the bilayer normal D_i, which is twice the travel of a single methylene group and has a maximal value of $D_M = 2.54$ Å. D_C can be calculated from the order parameters obtained for the plateau region carbon segments. As discussed elsewhere (20), D_C can be expressed by

$$D_C = \frac{1}{2}n_C D_M\left\langle\frac{1}{\cos\beta}\right\rangle^{-1}, \quad (6)$$

and

$$\left\langle\frac{1}{\cos\beta}\right\rangle \approx 3 - 3\langle\cos\beta\rangle + \langle\cos^2\beta\rangle. \quad (7)$$

Here β is β_i, which is the angle between the vector connecting the two neighboring carbons of the segment i relative to the bilayer normal.

Now, we need the values of $\langle\cos\beta_i\rangle$ and $\langle\cos^2\beta_i\rangle$, which are related to the first and second moments M_1 and M_2, respectively. In the liquid-crystalline state, they are obtained directly from the measured $S_{CD}^{(i)}$ order parameters. The calculation of $\langle\cos^2\beta_i\rangle$ is straightforward and is given by

$$\langle\cos^2\beta_i\rangle = \frac{1 - 4S_{CD}^{(i)}}{3}. \quad (8)$$

However, the calculation of $\langle\cos\beta_i\rangle$ is more complicated since $\langle\cos^2\beta_i\rangle^{1/2} \neq \langle\cos\beta_i\rangle$. To correlate $\langle\cos\beta_i\rangle$ with $\langle\cos^2\beta_i\rangle$ a model describing the population of all possible tilt angles β_i is required. Within the framework of a mean-torque model for the segmental distribution function an analytical solution for $\langle\cos\beta_i\rangle$ can be obtained, leading to (20):

$$\langle\cos\beta_i\rangle = \frac{1}{2}\left(1 + \sqrt{\frac{-8S_{CD}^{(i)} - 1}{3}}\right). \quad (10)$$

Note that the above result is only applicable for $S_{CD}^{(i)} \leq -1/8$ and uses the plateau values of the order parameter. The first-order mean-torque potential used for the calculations in this article is superior to other descriptions, such as the diamond lattice model (21).

RESULTS

Ultracentrifugal analysis of subunit *c* in octylglucoside micelles

Analytical ultracentrifuge experiments were carried out for evaluation of the size and distribution of subunit *c* oligomers in OG micelles. The sedimentation experiments gave rise to a single major component at 4 S as shown in Fig. 1 *a*. From the sedimentation equilibrium experiment shown in Fig. 1 *b*, an

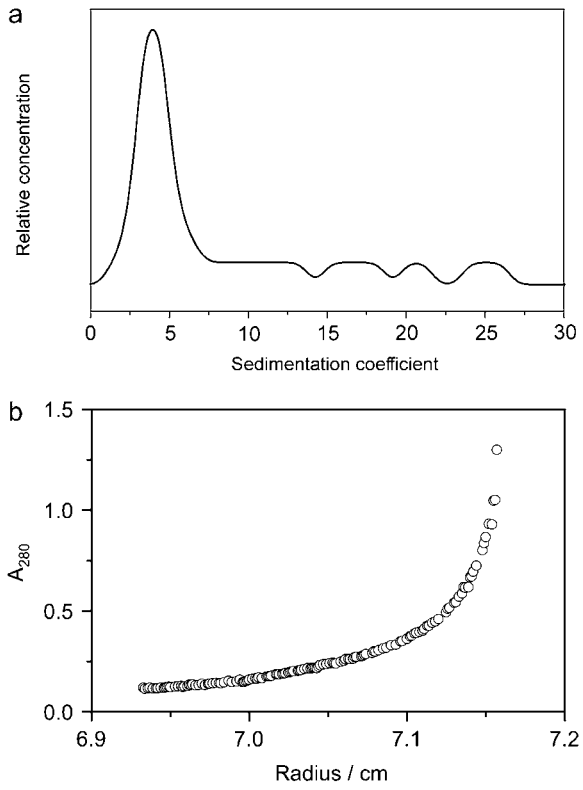

FIGURE 1 Analytical ultracentrifugation of subunit *c* in OG solution above the critical micelle concentration at 20°C. Protein concentration in the cell was scanned using ultraviolet light at 280 nm. (*a*) Distribution of sedimentation coefficient obtained in the sedimentation velocity experiment at 35,000 rpm for 1 h. (*b*) Sedimentation equilibrium experiment at 12,000 rpm for 24 h.

apparent molecular weight was estimated according to the equation,

$$\frac{d(\ln C)}{d(r^2)} = \frac{\omega^2 M(1 - \bar{v}\rho)}{2RT}, \quad (11)$$

where r is the radial position in the centrifugation cell, C is the concentration of the protein at distance r, $\bar{v}$ is the partial specific volume calculated from amino acid composition of subunit *c*, and ρ is the solvent density. Several analytical models can be applied to the curve shown in Fig. 1 *b*. On the basis of single component analysis, the apparent molecular weight for the detergent-bound protein was estimated to be 142,000. The molecular weight of subunit *c* is 8284. The contribution of the detergent molecules to this mixed micelle is not known, although the molecular weight of OG micelles is reported to be in the range 8000–29,000 (25,26).

Furthermore, self-assembly of the subunit *c*-ring in detergent solution has been reported (27). In view of the single major component in the sedimentation profile, the formation of uniform oligomers of subunit *c* in OG micelles can be concluded. This suggests formation of a *c*-ring in the order of decamer in the reconstituted membranes (28).

^{2}H-NMR spectra of the subunit *c*-reconstituted membranes

^{2}H-NMR powder pattern spectra were obtained for DMPC-d_{54} membranes in the absence and presence of subunit *c* at various temperatures as shown in Fig. 2 *a*. The membranes at molar lipid/protein ratios of 50:1 and 20:1 were investigated. The ^{2}H-NMR spectra changed significantly with the temperature. At 30°C the results for the three membrane samples were similar to one another and indicated that they were in the liquid-crystalline phase (19). The splittings represent a set of RQCs corresponding to the different segments of the deuterated acyl chains. As the temperature decreased, the line shape was broadened substantially, and the distinct quadrupolar splittings became unresolved. At 18°C, the spectrum of DMPC-d_{54}/subunit *c* (20:1) lost the resolved pattern in contrast to those of DMPC-d_{54} and DMPC-d_{54}/subunit *c* (50:1) membranes. In the gel state below 15°C, the individual splittings disappeared and the spectra of all three samples had a triangular shape. The spectral width extended to ±60 kHz, with an additional small splitting arising from the terminal C^2H_3 groups. At −60°C, broad powder patterns with intensity maxima at ±60 kHz and with rotating methyl signals were observed (spectra not shown).

Fig. 2, *b–d*, presents theoretical spectra calculated as benchmarks for various limiting types of motions that can average the static quadrupolar coupling (19). In the liquid-crystalline state, a crankshaft-type motion corresponds to an infinite polymethylene chain saturated with *trans-gauche*$^{\pm}$–*trans-gauche*$^{\mp}$ pairs, with three-site jumps of the C–^{2}H-bonds on a tetrahedral lattice with equal populations. The axis for the jumps sites is inclined at $\theta = 109.47°$ relative to the symmetry axis of the electric field gradient (EFG) tensor, giving $P_2(\cos\theta) = -1/3$ (19). Fig. 2 *b* depicts the theoretical powder-type ^{2}H-NMR spectrum for a crankshaft model with spectral discontinuities at ±20.875 kHz and ∓ 41.75 kHz. In the gel state, one can analogously consider as a benchmark the case of two-site jumps, corresponding to restricted isomerization, which yields a totally asymmetric spectrum with discontinuities at 0, ±62.625 kHz (29) (not shown). By contrast, continuous or threefold rotation of all-*trans* polymethylene chains, where the rotational axis is at $\theta = 90°$ to the largest EFG principal axis, is axially symmetric, giving $P_2(\cos\theta) = -1/2$. Fig. 2 *c* shows the theoretical ^{2}H-NMR spectrum corresponding to the rotation of lipid molecules around the long axis parallel to the membrane normal, yielding discontinuities at ±31.313 kHz and ∓ 62.625 kHz. Lastly, when the rotation is ''frozen'' on the ^{2}H-NMR timescale, the ^{2}H-NMR line shape represents a static powder pattern as shown in Fig. 2 *d*, with discontinuities at about ±62.625 kHz and ∓ 125.25 kHz.

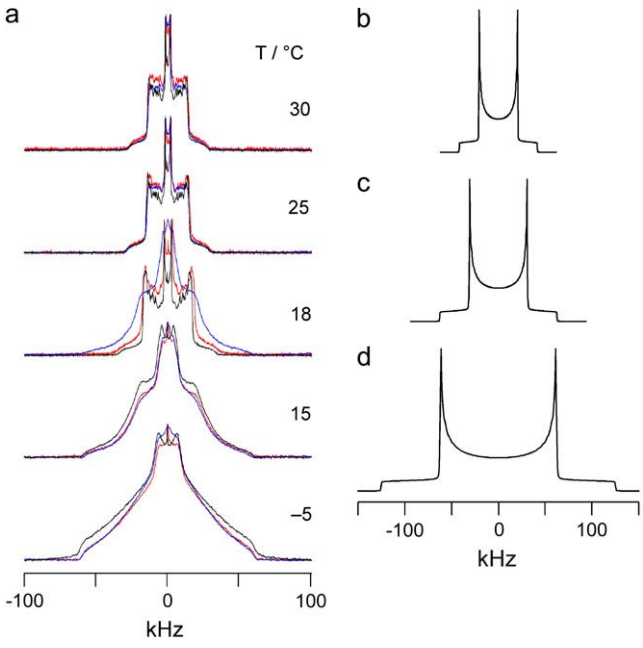

FIGURE 2 ^{2}H-NMR powder pattern spectra of multilamellar liposomes. (*a*) Experimental ^{2}H-NMR of fully hydrated DMPC-d_{54} membranes (*black line*), DMPC-d_{54}/subunit *c* membranes (50:1 molar ratio) (*red line*), and DMPC-d_{54}/subunit *c* (20:1) membranes (*blue line*) at 30°C, 25°C, 18°C, 15°C, and −5°C. On the left, theoretical spectra for (*b*) equally probable three-site jumps corresponding to crankshaft motion of polymethylene chains or threefold rotation of methyl groups on static chain ($\langle\chi_Q\rangle = -1/3\,\chi_Q$), (*c*) rotation of all-*trans* polymethylene chain ($\langle\chi_Q\rangle = -1/2\chi_Q$), and (*d*) rigid limit ($\chi_Q = 167$ kHz).

With these spectra as benchmarks, we can thus see that in the gel phase at 15°C and below ^{2}H-NMR spectral intensity is evident at ±60 kHz. The spectra increasingly adopt a triangular shape, excepting the central C^2H_3 component, which might be indicative of a contribution from two-site jump isomerization. On the other hand, little evidence for axial diffusion of the chains is apparent, indicating they are highly entangled. The ^{2}H-NMR spectra at −5°C and 15°C are also broadened, indicating the occurrence of motions at intermediate timescales.

Moment analysis of ^{2}H-NMR powder pattern spectra

First and second moments of the ^{2}H-NMR spectra of the three DMPC-d_{54} membrane samples as a function of decreasing temperature are presented in Fig. 3. Spectra were obtained for both decreasing and increasing temperature, and the processes were found to be essentially reversible for the three membrane systems investigated. As temperature decreases, the first and second moment values for all three membranes increase. A phase transition occurred from the liquid-crystalline (L_α) to the gel state at around 18°C, which is somewhat lower than for nondeuterated DMPC (23°C) due to the ^{2}H-isotope effect. Although line broadening in the ^{2}H-NMR spectrum of DMPC-d_{54}/subunit *c* (20:1) at 18°C was noticeable in Fig. 2 *a*, the phase transition temperature changed little in the moment plots. In the liquid-crystalline state, the first and second moments are similar for the three membrane samples. In contrast, the moments are smaller in the presence

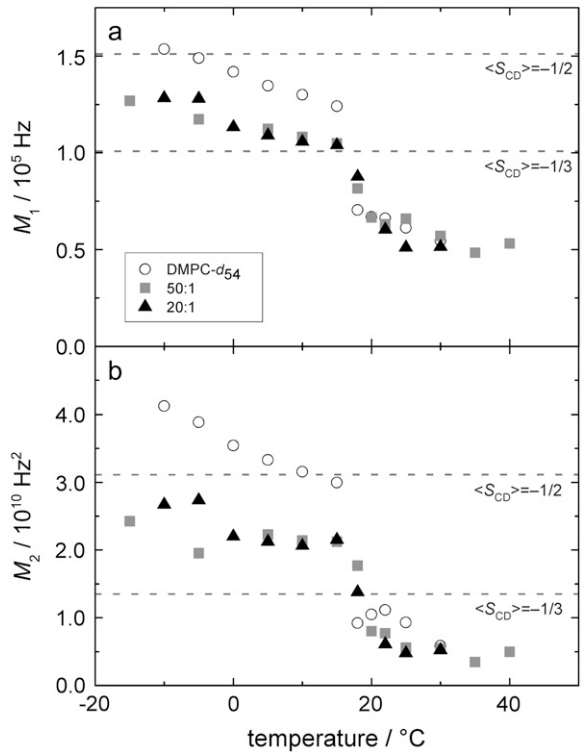

FIGURE 3 Plots of (*a*) the first moment (M_1) and (*b*) the second moment (M_2) of the ^{2}H-NMR spectra as a function of temperature on decrease. The error is given by the size of the symbol. Spectra were acquired with decreasing temperature. Dotted lines correspond to the moment values calculated for average order parameters of −1/2 (Fig. 2 *c*) and −1/3 (Fig. 2 *b*).

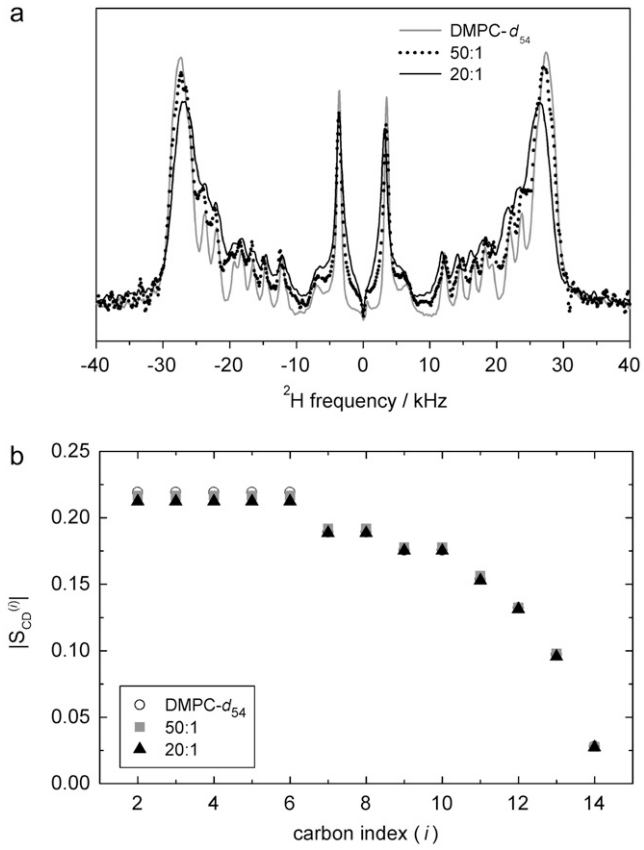

FIGURE 4 (*a*) De-Paked ^{2}H-NMR spectra of DMPC-d_{54}, DMPC-d_{54}/subunit *c* (50:1), and DMPC-d_{54}/subunit *c* (20:1) membranes at 30°C. (*b*) The segmental order parameter of the C–^{2}H-bond in the fatty acid chains as a function of carbon number *i* at 30°C. The error is given by the size of the symbol.

of subunit *c* in the gel state, suggesting that the proteins induce more disorder in the lipid bilayers.

As the temperature decreases, the moments M_1 and M_2 become larger. The first and second moments are correlated to the average order parameter and the mean-squared order parameter, respectively, as given by Eqs. 4 and 5. Therefore, the average orientational order of the C–^{2}H-bonds increases with decrease in temperature. For comparison, the moments calculated for all-*trans* rotation ($S_{CD} = -1/2$) and a crankshaft model, which involves three-site jump isomerization ($S_{CD} = -1/3$), are indicated as dotted lines. The moment and spectral line shape analyses show that the crankshaft motion of methylene chain is not enough to explain fluidity in the liquid-crystalline L_α phase.

Order parameters of C-D bonds in the subunit *c*-reconstituted membranes

A detailed analysis of order parameters was performed for the resolved segment positions of the deuterated hydrocarbon chains of DMPC-d_{54} in the liquid-crystalline state. Fig. 4 *a* reveals representative ^{2}H-de-Paked spectra of DMPC-d_{54} membranes in the absence and presence of subunit *c* at 30°C. The de-Paked ^{2}H-NMR spectrum represents the bilayer normal aligned parallel to the magnetic field, corresponding to the average orientation of the lipid molecules. Nine resolved residual quadrupolar splittings could be clearly observed. Assignments were made following a previous work (30). The largest splitting was assigned to the C2–C6 methylene carbons of the *sn*-1 chain and C3–C6 carbons of the *sn*-2 chain. The progressively decreasing splittings were assigned to the C7 to terminal methyl groups of the acyl chains, respectively.

The order parameter obtained from the splitting was plotted in Fig. 4 *b* only for the *sn*-1 chain for simplicity. The profile was similar for the *sn*-2 chain. The largest order parameters in the plateau region were almost −0.22 for all membrane samples (Fig. 4 *b*). This value is almost identical to the previously reported one. This is smaller in absolute magnitude than that for the benchmark crankshaft model ($S_{CD} = -1/3$). Consequently, the motions even in the most rigid part of the acyl chains are more disordered than the three-site jump crankshaft motions. Subunit *c* induced a slight decrease only in the largest quadrupolar splitting, indicating that it must interact with the fluid phospholipid chains in a manner that preserves their fluid properties. As the fraction of subunit *c* in the bilayer increased, the spectral

resolution became lower. However, the order parameters did not change significantly. The segmental order parameters are plotted as a function of carbon number in Fig. 4 *b* for the three membrane samples at 30°C. The $S_{CD}^{(i)}$ values decrease toward the methyl termini of the chains and approach the isotropic limit ($S_{CD} = 0$) in the bilayer center, showing a liquid-like property. The effect of subunit *c* is small, especially in the center of the bilayer.

The ^{31}P-NMR spectrum was also observed at 30°C for monitoring the effect on the polar headgroup. It gave a typical axial symmetric powder pattern in accordance with the bilayer structure in the liquid-crystalline state. Introduction of subunit *c* induced a small line-broadening but no significant change in the chemical shift anisotropy (spectra not shown).

Spin-lattice relaxation rates of the deuterons in fatty acid chains in the subunit *c*-reconstituted membranes

To explore the dynamic properties of the subunit *c*-reconstituted membranes, the spin-lattice relaxation rates of the deuterons of the hydrocarbon chains were measured. Partially relaxed ^{2}H-NMR spectra of DMPC-d_{54}/subunit *c* (50:1) in the de-Paked form at 30°C are presented in Fig. 5 *a*. Note that the relaxation rate for inversion recovery increases as the residual quadrupolar splitting becomes larger. The largest splitting corresponds to the C2–C6 methylene carbons and recovers in <20 ms. The smaller splittings recover with a longer delay time; in particular the smallest splitting of the methyl resonance takes more than 200 ms for the inversion recovery. The ^{2}H-spin-lattice relaxation rate, $R_{1Z}^{(i)}$, at 30°C is plotted as a function of the chain carbon number for the three membrane samples in Fig. 5 *b* for the *sn*-1 chain. The values show a plateau that is reminiscent of the corresponding order profile, and they decrease from the carbonyl side to the methyl terminus of the chain. The effect of subunit *c* on $R_{1Z}^{(i)}$ was small but evident in contrast to the case of order parameters at the same temperature.

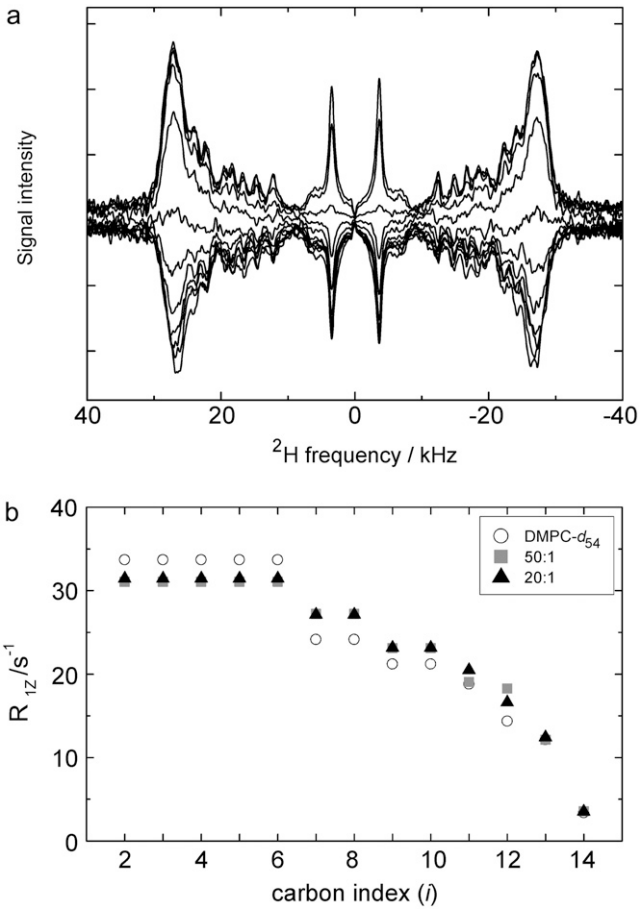

FIGURE 5 (*a*) Partially relaxed de-Paked ^{2}H-NMR spectra of DMPC-d_{54}/subunit *c* (50:1) at 30°C. Values of inversion-recovery delay τ are 0.2, 0.5, 1, 2, 5, 10, 20, 50, 100, 200, 500, and 1000 ms from bottom to top. (*b*) The profile of ^{2}H-spin-lattice relaxation rates $R_{1Z}^{(i)}$ as a function of segmental position *i* for DMPC-d_{54}, DMPC-d_{54}/subunit *c* (50:1), and DMPC-d_{54}/subunit *c* (20:1) membranes at 30°C. Their errors were ~9%, 7%, and 4%, respectively.

DISCUSSION

The centrifugal analysis of subunit *c* in OG micelles clearly shows that it forms a well-defined oligomer in the micelles. This result suggests that the subunit *c* oligomer adopts a ring structure in the reconstituted membranes as shown for the V-type ATPase *K*-ring (7) and F-type Na^+-ATP synthase *c*-ring (6). The *c*-ring in *E. coli* F_o has been reported to be a decamer of subunit *c* molecules (4). Thus, this work can provide information regarding interactions between the subunit *c*-ring and the surrounding lipid bilayers.

In solid-state ^{2}H-NMR, the order parameters and corresponding first moments are related to the volumetric thickness of the membrane. In the L_α phase of DMPC, the first and second moments were not affected by the presence of subunit *c* within experimental errors, suggesting matching of the membrane thickness to the hydrophobic region of subunit *c*. A simple question would arise. Do these samples really include the subunit *c*? The presence of subunit *c* was confirmed as described in Materials and Methods. It can also be confirmed by the ^{2}H-NMR spectra of those in the gel state (Figs. 2 and 3). Furthermore, a well-defined cross-polarization/MAS ^{13}C-NMR spectrum of subunit *c* could be obtained for the sample with the uniformly ^{13}C-labeled subunit *c* prepared in the same way (Y. Todokoro, M. Kobayashi, T. Fujiwara, and H. Akutsu, unpublished result). Thus, we are sure that the subunit *c*-ring is embedded in the membrane homogeneously. Then, we calculated a hydrocarbon thickness of the DMPC bilayer using Eqs. 6–10.

The obtained value was 26 Å at 30°C. The thickness was little affected by the presence of subunit *c*, even at very high molar ratios of 50:1 and 20:1. The value of the thickness is in good agreement with that reported of the hydrocarbon core of the DMPC bilayer, 26 Å (13,20,32). In the gel state, however, the thickness of the DMPC-d_{54} membranes in-

cluding subunit *c* is thinner than that for DMPC-d_{54} membranes in its absence. This indicates a mismatch of the membrane thickness to the hydrophobic interface of subunit *c*. Hydropathy analysis (33) can be used to estimate the length of the hydrophobic surface of subunit *c* across the membrane. Its hydrophobic length can be compared to the bilayer dimensions determined on the ^{2}H-NMR analysis. The charged residues (34) are colored red and blue in the structure of subunit *c* from *E. coli*. (Protein Data Bank: 1A91) in Fig. 6 *b*.

According to this, the hydrophobic thickness of subunit *c* is close to that of the bilayer in the liquid-crystalline state (26 Å) but is much smaller than that in the gel state (~32 Å). The difference in the hydrophobic thickness between the protein and the lipid bilayers in the gel state will induce a disorder in the lipid molecules around subunit *c*. The hydrophobic matching in the L_α phase has been reported for membrane proteins and lipid bilayers. For example, *E. coli* and *Mycobacterium tuberculosis* MscLs (mechanosensitive channel of large conductance) were shown to have the highest affinity with dipalmitoleoyl phosphatidylcholine (PC) and dimryristoleoyl PC among unsaturated PCs with different carbon numbers (35); and the hydrophobic thickness of MscL in the unsaturated PC membrane was found to be 25 Å

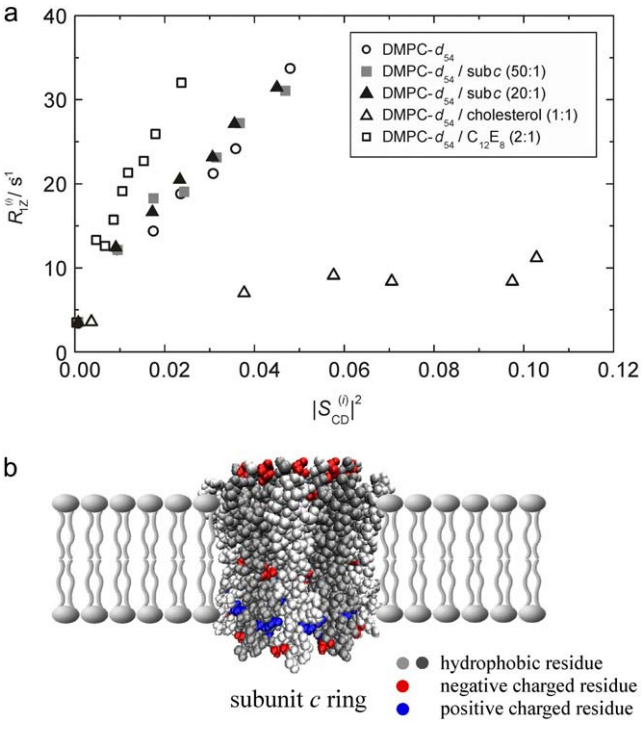

FIGURE 6 (*a*) $R_{1Z}^{(i)}$ plots as a function of $|S_{CD}^{(i)}|^2$ for DMPC-d_{54}, DMPC-d_{54}/subunit *c* (50:1), and DMPC-d_{54}/subunit *c* (20:1) membranes at 30°C. Reference data for DMPC-d_{54}/cholesterol (1:1) (30) and DMPC-d_{54}/$C_{12}E_8$ (2:1) (39) are also presented. (*b*) A schematic model of the *c*-ring in lipid bilayers in the liquid-crystalline state. A solution structure of EF_o subunit *c* (41) was used. Charged amino acid residues are highlighted in the structure of the subunit *c*-ring (Glu and Asp in *red*, and Lys and Arg in *blue*).

(36). This is in good agreement with our result. Therefore, the hydrophobic matching found in this work will have physiological significance.

Let us turn to the effect of subunit *c* on the spin-lattice relaxation rates in the liquid-crystalline state. The relaxation mechanism of deuterons in lipid bilayers is governed by segmental motions such as exchange of *trans-gauche* conformations, motions of the centers of mass of the flexible molecules within the bilayer or collective motions of the bilayer lipids (37). To investigate the effect of subunit *c* on viscoelastic properties of the membrane, $R_{1Z}^{(i)}$ was plotted as a function of $|S_{CD}^{(i)}|^2$ as shown in Fig. 6 *a*. DMPC bilayers in the absence of subunit *c* revealed a linear relationship as reported earlier (37). This is explained by its viscoelastic behavior; i.e., the relaxation is governed by relatively slow fluctuations of the RQC averaged over local segmental motions of the bilayer lipids, which are further modulated by slower bilayer disturbances associated with their viscoelastic behavior of the membrane lipids. The slope represents the softness of the lipid bilayers, viz. the viscoelastic behavior on a mesoscopic distance scale (37,38).

The influence of subunit *c* on the plots is small, suggesting that the hydrophobic matching of subunit *c* is realized not only for the bilayer thickness but also for the softness in the liquid crystalline state. This is in sharp contrast to effects of other bilayer additives such as cholesterol and cosurfactants or detergents. The relaxation rates in the presence of cholesterol and nonionic detergent ($C_{12}E_8$) (30,39) are presented in Fig. 6 *a* for comparison. These relaxation rates are also proportional to $|S_{CD}^{(i)}|^2$. The slope of the square-law plot for the DMPC-d_{54}/$C_{12}E_8$ (2:1) mixed bilayer is much steeper than that for DMPC-d_{54}/cholesterol (1:1) membrane. This indicates that cholesterol stiffens and $C_{12}E_8$ softens the DMPC-d_{54} membranes in accord with their macroscopic effects on the bilayers. On the contrary, the average slope for DMPC-d_{54}/subunit *c* membranes is similar to that for DMPC-d_{54} bilayers. This means that the interactions between lipids and the surface of the subunit *c*-ring is soft and well matched, resulting in small perturbations to the lipid bilayers. However, a close inspection of the plots reveals an effect of the additive to the membrane properties.

The methylenes in the bilayer central core show a steeper slope for the subunit *c*/DMPC bilayers than for DMPC bilayers, whereas near the top of the chain the influence of subunit *c* is less. This is typical behavior for inhomogeneous lipid bilayers (40) and suggests that the central part of DMPC in the presence of subunit *c* is softer than the pure DMPC bilayers. Recently the crystal structures of the K-ring of V-type ATPase (7) and the *c*-ring of Na^+-ATP synthase were reported (6). The hairpin structure shows a bend in the center in the ring structures in crystal as well as in solution. This provides an inward curvature on the outer surface of the ring with the shortest diameter at the center of the membrane. It will offer more space to the disordered part of the hydrocarbon chains. This may be one reason that the lipids are

softer in the center than in the region of the interface to the polar groups.

Our results clearly indicat that subunit *c* interacts with the lipids in nearly the same manner that the flexible lipids interact among themselves in the liquid-crystalline state. This is achieved by their matching in the thickness. A mismatch introduces disorder in the lipid molecules around subunit *c*, which can be the origin of strong friction between the protein and the lipid bilayer. Furthermore, the soft interactions between the *c*-ring and flexible hydrocarbon chains would be important for exerting functions of subunit *c*. In F_1F_o-ATP synthase embedded in membranes, a subunit *c* in the *c*-ring receives H^+ from the proton channel in one side of the membrane. Then, the *c*-ring has to rotate in the lipid membrane to release the proton to the proton channel in the other side of the membrane. The thickness matching and soft interactions between the *c*-ring and lipid bilayers mentioned above should make this rotation smooth with a minimal loss of energy by friction. This would contribute to the high-speed rotation of the *c*-ring in F_o and the $\gamma\varepsilon$ subunit axle in F_1 for efficient ATP synthesis and hydrolysis. Any significant degree of hydrophobic mismatch could lead to membrane deformation that could alter the rotation of the *c*-ring within the bilayer. Indeed, F_1F_o-ATP synthase from thermophilic *Bacillus* is active in DMPC bilayers in the liquid-crystalline state (T. Suzuki and M. Yoshida, Tokyo Institute of Technology, personal communication, 2006).

CONCLUSION

^{2}H-NMR spectroscopy provided direct information on the interactions between the subunit *c*-ring and lipid bilayers. The hydrophobic length of subunit *c* appeared to be similar to that of DMPC bilayers in the liquid-crystalline state but less than that in the gel state. From the dynamic point of view, ^{2}H-NMR relaxation profiles showed a fluid mechanical matching of the lipid bilayers to subunit *c* in the liquid-crystalline state. Therefore, the hydrophobic matching can be accounted for by at least two factors: the hydrophobic length and the fluid mechanical property. The hydrophobic matching between subunit *c* and DMPC bilayers is realized in the liquid-crystalline state, where F_1F_o-ATP synthase is active.

We thank Profs. R. H. Fillingame and M. Yoshida for providing us *E. coli* MEG119 strain transformed by plasmid pCP35 and Dr. G. Martinez for the computer programs used for spectral analysis. We are grateful to Ms. M. Sakai for her help in ultracentrifugation experiments and to Dr. Y. Todokoro for discussions.

M.F.B. was a JSPS fellow. This work was partly supported by Grants-in-Aid for Scientific Research on Priority Areas and the Target Protein Project from MEXT Japan (H.A.) and grants from the U.S. National Institutes of Health (M.F.B.).

REFERENCES

1. Boyer, P. D. 1997. The ATP synthase—a splendid molecular machine. *Annu. Rev. Biochem.* 66:717–749.
2. Yoshida, M., E. Muneyuki, and T. Hisabori. 2001. ATP synthase—a marvellous rotary engine of the cell. *Nat. Rev. Mol. Cell Biol.* 2:669–677.
3. Miller, M. J., M. Oldenburg, and R. H. Fillingame. 1990. The essential carboxyl group in subunit c of the F_1F_o ATP synthase can be moved and H^+-translocating function retained. *Proc. Natl. Acad. Sci. USA.* 87:4900–4904.
4. Jiang, W., J. Hermolin, and R. H. Fillingame. 2001. The preferred stoichiometry of *c* subunits in the rotary motor sector of *Escherichia coli* ATP synthase is 10. *Proc. Natl. Acad. Sci. USA.* 98:4966–4971.
5. Mitome, N., T. Suzuki, S. Hayashi, and M. Yoshida. 2004. Thermophilic ATP synthase has a decamer *c*-ring: indication of noninteger 10:3 H^+/ATP ratio and permissive elastic coupling. *Proc. Natl. Acad. Sci. USA.* 101:12159–12164.
6. Meier, T., P. Polzer, K. Diederichs, W. Welte, and P. Dimroth. 2005. Structure of the rotor ring of F-type Na^+-ATPase from *Ilyobacter tartaricus*. *Science.* 308:659–662.
7. Murata, T., I. Yamato, Y. Kakinuma, A. G. W. Leslie, and J. E. Walker. 2005. Structure of the rotor of the V-type Na^+-ATPase from *Enterrococcus hirae*. *Science.* 308:654–659.
8. Seelert, H., A. Poetsch, N. A. Dencher, A. Engel, H. Stahlberg, and D. J. Müller. 2000. Proton-powered turbine of a plant motor. *Nature.* 405:418–419.
9. Meier, T., U. Matthey, C. von Ballmoos, J. Vonck, T. K. von Nidda, W. Kühlbrandt, and P. Dimroth. 2003. Evidence for structural integrity in the undecameric *c*-ring isolated from sodium ATP synthase. *J. Mol. Biol.* 325:389–397.
10. Rastogi, V. K., and M. E. Girvin. 1999. Structural changes linked to proton translocation by subunit c of the ATP synthase. *Nature.* 402: 263–268.
11. Nakano, T., T. Ikegami, T. Suzuki, M. Yoshida, and H. Akutsu. 2006. A new solution structure of ATP synthase subunit *c* from *Thermophilic bacillus* PS3, suggesting a local conformational change for H^+-translocation. *J. Mol. Biol.* 358:132–144.
12. Junge, W., and N. Nelson. 2005. Nature's rotary electromotors. *Science.* 308:642–644.
13. Nagle, J. F., and S. Tristan-Nagle. 2000. Structure of lipid bilayers. *Biochim. Biophys. Acta.* 1469:159–195.
14. Girvin, M. E., and R. H. Fillingame. 1993. Helical structure and folding of subunit *c* of F_1F_o ATP synthase: ^{1}H NMR resonance assignments and NOE analysis. *Biochemistry.* 32:12167–12177.
15. Girvin, M. E., and R. H. Fillingame. 1995. Determination of local protein structure by spin label difference 2D NMR: the region neighboring Asp61 of subunit *c* of the F_1F_o ATP synthase. *Biochemistry.* 34:1635–1645.
16. Bloom, M., J. H. Davis, and A. L. MacKay. 1981. Direct determination of the oriented sample NMR spectrum from the powder spectrum for systems with local axial symmetry. *Chem. Phys. Lett.* 80:198–202.
17. McCabe, M. A., and S. R. Wassall. 1995. Fast-Fourier-transform dePaking. *J. Magn. Reson. B.* 106:80–82.
18. Davis, J. H. 1983. The description of membrane lipid conformation, ordered and dynamics by ^{2}H-NMR. *Biochim. Biophys. Acta.* 737: 117–171.
19. Brown, M. F. 1996. Membrane structure and dynamics studied with NMR spectroscopy. *In* Biological Membranes. K. M. Merz Jr. and B. Roux, editors. Birkhauser, Boston, MA. 175–252.
20. Petrache, H. I., S. W. Dodd, and M. F. Brown. 2000. Area per lipid and acyl length distributions in fluid phosphatidylcholines determined by ^{2}H NMR spectroscopy. *Biophys. J.* 79:3172–3192.
21. Salmon, A., S. W. Dodd, G. D. Williams, J. M. Beach, and M. F. Brown. 1987. Configurational statistics of acyl chains in polyunsaturated lipid bilayers from ^{2}H NMR. *J. Am. Chem. Soc.* 109:2600–2609.
22. Jansson, M., R. L. Thurmond, J. A. Barry, and M. F. Brown. 1992. Deuterium NMR study of intermolecular interactions in lamellar phases containing palmitoyllysophosphatidylcholine. *J. Phys. Chem.* 96:9532–9544.

23. Henzler-Wildman, K. A., G. V. Martinez, M. F. Brown, and A. Ramamoorthy. 2004. Perturbation of the hydrophobic core of lipid bilayers by the human antimicrobial peptide LL-37. *Biochemistry*. 43:8459–8469.

24. Vogel, A., C. P. Katzka, H. Waldmann, K. Arnold, M. F. Brown, and D. Huster. 2005. Lipid modifications of a Ras peptide exhibit altered packing and mobility versus host membrane as detected by 2H solid-state NMR. *J. Am. Chem. Soc.* 127:12263–12272.

25. Lorber, B., J. B. Bishop, and L. J. DeLukas. 1990. Purification of octyl β-D-glucopyranoside and re-estimation of its micellar size. *Biochim. Biophys. Acta*. 1023:254–265.

26. le Maire, M., P. Champeil, and J. V. Moller. 2000. Interaction of membrane proteins and lipids with solubilizing detergents. *Biochim. Biophys. Acta*. 1508:86–111.

27. Arechaga, I., P. J. G. Butler, and J. E. Walker. 2002. Self-assembly of ATP synthase subunit *c* rings. *FEBS Lett*. 515:189–193.

28. Fillingame, R. H., and O. Y. Dmitriev. 2002. Structural model of the transmembrane F_o rotary sector of H^+-transporting ATP synthase derived by solution NMR and intersubunit cross-linking *in situ*. *Biochim. Biophys. Acta*. 1565:232–245.

29. Huang, T. H., R. P. Skarjune, R. J. Wittebort, R. G. Griffin, and E. Oldfield. 1980. Restricted rotational isomerization in polymethylene chains. *J. Am. Chem. Soc.* 102:7377–7379.

30. Trouard, T. P., A. A. Nevzorov, T. M. Alam, C. Job, J. Zajicek, and M. F. Brown. 1999. Influence of cholesterol on dynamics of dimyristoylphosphatidylcholine bilayers as studied by deuterium NMR relaxation. *J. Chem. Phys.* 110:8802–8818.

31. Reference deleted in proof.

32. Cornell, B. A., and F. Separovic. 1983. Membrane thickness and acyl chain length. *Biochim. Biophys. Acta*. 733:189–193.

33. Huber, T., A. V. Botelho, K. Beyer, and M. F. Brown. 2004. Membrane model for the G-protein-coupled receptor rhodopsin: hydrophobic interface and dynamical structure. *Biophys. J.* 86:2078–2100.

34. Wimly, W. C., and S. H. White. 1996. Experimentally determined hydrophobicity scale for proteins at membrane interfaces. *Nat. Struct. Biol.* 3:842–848.

35. Powl, A. M., J. M. East, and A. G. Lee. 2003. Lipid-protein interactions studied by introduction of a tryptophan residue: the mechanosensitive channel MscL. *Biochemistry*. 42:14306–14317.

36. Powl, A. M., J. N. Wright, J. M. East, and A. G. Lee. 2005. Identification of the hydrophobic thickness of a membrane protein using fluorescence spectroscopy: studies with the mechanosensitive channel MscL. *Biochemistry*. 44:5713–5721.

37. Brown, M. F., R. L. Thurmond, S. W. Dodd, D. Otten, and K. Beyer. 2002. Elastic deformation of membrane bilayers probed by deuterium NMR relaxation. *J. Am. Chem. Soc.* 124:8471–8484.

38. Brown, M. F., R. L. Thurmond, S. W. Dodd, D. Otten, and K. Beyer. 2001. Composite membrane deformation on the mesoscopic length scale. *Phys. Rev. E Stat. Nonlin. Soft Matter Phys.* 64:10901–10904.

39. Otten, D., M. F. Brown, and K. Beyer. 2000. Softening of membrane bilayers by detergents elucidated by deuterium NMR spectroscopy. *J. Phys. Chem. B*. 104:12119–12129.

40. Rajamoorthi, K., H. I. Petrache, T. J. McIntosh, and M. F. Brown. 2005. Packing and viscoelasticity of polyunsaturated ω-3 and ω-6 lipid bilayers as seen by ^2H NMR and x-ray diffraction. *J. Am. Chem. Soc.* 127:1576–1588.

41. Girvin, M. E., V. K. Rastogi, F. Abildgaard, J. L. Markley, and R. H. Fillingame. 1998. Solution structure of the transmembrane H^+-transporting subunit *c* of the F_1F_o ATP synthase. *Biochemistry*. 37:8817–8824.